

Oxidation of Simple and Pt- Modified Diffusion Coating on Inconel Alloy 600 in Air

Ahmed Ali Moosa,* Hussein Al-Alqawie,*
Khalil Al-Hatab*

Received on:15/2/2005

Accepted on:18/7/2005

Abstract

In this work the oxidation behavior of both Inconel alloy 600 and coated system (Pt-modified aluminide coating) was investigated in air in the temperatures range 700 - 1000 °C. The oxidation kinetic of inconel alloy 600 and its coated system was found to follow the parabolic law. Large voids were found at the oxide scales-substrate interface and at grains or at grain boundaries. This is due to the chromium depletion in the alloy. The mechanism of void formation has often been attributed to the vacancy condensation.

Inconel alloy 600 was coated with Pt-modified aluminide using single-step high activity pack cementation method. At 900 °C, the parabolic rate constant is 6.63×10^{-7} for the coated system and 1.16×10^{-6} ($\text{mg}^2 / \text{cm}^4 \cdot \text{sec}$) for the uncoated system. Oxide phases that are formed on coated system during most of the oxidation exposure conditions are: Al_2O_3 , NiAl_2O_4 , Cr_2O_3 , and NiFe_2O_4 .

Key-words: Oxidation, Diffusion coating, Pack cementation, Inconel alloy.

أكسدة سباتك انكونيل-600 المحوره بالطلاء الانتشاري الالمنه-بلاتين

الخلاصة

تم دراسة سلوك الأكسدة لسبيكة انكونيل (inconel alloy 600) وسبيكة انكونيل التي تم طلاؤها كهروكيميائيا بسبالتين ثم الطلاء بالسمنتة Pack Cementation Technique لترسيب الألومنيوم عليها في درجة حرارة 1034°C . تمت دراسة سلوك الأكسدة للأنظمة أعلاه في الهواء عند درجات حرارة هي $700-1000^\circ\text{C}$. تشير النتائج ان السلوك العام للتأكسد لسبيكة الانكونيل غير المطيلية والمطيلية يتبع تقريبا قانون القطع المكافئ k_p Parabolic. تشير النتائج الى تكون فجوات كبيرة عند السطح الفاصل بين الأوكسيد وسبيكة الأساس كنتيجة لتجمع الفجوات الذرية vacancies والتي تنتج عملية التأكسد لعناصر السبيكة كالكروم.

أخيرا، تمت دراسة سلوك التأكسد لنظام الطلاء (سبيكة انكونيل 600 / الألومينايد المدعم بالبلاتينيوم) في الهواء وعند درجة حرارة 900°C أن قيم k_p لنظام الطلاء هي 6.63×10^{-7} مقارنة مع 1.16×10^{-6} ($\text{mg}^2 / \text{cm}^4 \cdot \text{sec}$) للسبيكة غير المطيلية. تشير نتائج التحليل بالأشعة السينية الى ظهور أكاسيد الكروم والنيكل إضافة الى أكسيد الألومنيوم كما يلي: NiFe_2O_4 , NiAl_2O_4 , Cr_2O_3 , Al_2O_3 .

Introduction

Aluminide diffusion coatings are commonly applied by pack cementation method to Ni-based

superalloy turbine components to improve their oxidation resistance. Nickel aluminide (NiAl) is the promising high temperature structural

* Dept. of Production Eng. & Metallurgy, UOT.

material because it has good properties, such as low density, high melting point (1640 °C) and good thermal conductivity. NiAl has excellent potential of oxidation resistance, due to its ability to form a protective α -Al₂O₃ scale and the ability to form a healing oxide after spallation [1]. However, aluminide coatings lack adequate resistance to hot corrosion (fused salt attack, e.g., Na₂ SO₄) and to thermal stresses generated during gas turbine service [2].

Aluminide coatings are carried out using either a low-activity high temperature (LAHT) or a high-activity low temperature (HALT) pack cementation. Conventionally, low-activity coating is developed in one step above 1000 °C for 3 to 4 hrs to produce a NiAl. High-activity aluminizing is carried out at 700 - to 850 °C, which is then followed by a diffusion treatment above 1000 °C to form NiAl coating structure [3].

The presence of platinum in nickel aluminide promotes the formation of a protective alumina scale. Consequently, the oxidation resistance of Pt- aluminide coatings is better than that of aluminide coatings without platinum [4]. A variety of mechanisms have been proposed to explain the beneficial effects of Pt [5-10].

Studies on the cyclic oxidation of CM-247 Ni-based cast superalloy with plain aluminide coating and with Pt- aluminide coating at 1000- 1200 °C in air show that Pt-aluminide coating improves the oxidation resistance. This is because of its ability to retain alumina as the only oxide phase and prevent spinel formation for much longer periods during oxidation than plain aluminide counterpart does [11].

The formation of α -Al₂O₃ from θ -Al₂O₃ on the β -NiAl coating resulted in a sharp decrease in the parabolic rate constant k_p by one order of magnitude [12]. Moreover the parabolic rate constant for the Pt-aluminide coating was nearly two orders of magnitude lower than that for the plain aluminide coating during isothermal oxidation of nickel superalloy CM-247 at 1100 °C [13]. The aim of this work is to study the effects of platinum-aluminide diffusion coating on oxidation of Ni superalloy (Inconel 600).

Materials and Methods

The spectrochemical analysis of Ni based superalloy (Inconel alloy 600) is shown in table 1 . Coupons of dimensions 2 cm × 2 cm × 0.4 cm with a total exposed area of 11.2 cm² were cut out from inconel 600 sheet. Small hole 1 mm in diameter was drilled in each coupon for holding. All the surfaces, including the edges were wet ground using 150, 300 and 600 grit silicon carbide papers. These samples were then cleaned in water, degreased with acetone, and then dried.

Pt-modified aluminide Coating

Pt-modified aluminide coating was produced on inconel alloy 600 substrates by using the following steps: (a) A thin Pt layer is produced by electroplating method. (b) Diffusion annealing treatment. (c) High activity aluminizing process. Each Inconel alloy 600 samples was coated electrochemically with platinum layer. A platinum plating solution consisted of Pt20-Q salt ([Pt (NH₃)₄] HPO₄ from Johnson Matthey Catalysts) electrolyte at 90-95°C with 10 g/l of Pt. The Pt thickness was ~2.5

μm after 15 min of plating time based on the mass gain.

The Pt-coated Inconel alloy 600 samples were then given diffusion annealing at 850°C for up to 0.5 hours and consequently the temperature was increased to 1034°C for up to 2 hours in a vacuum furnace at 10^{-3} torr.

Subsequently, the diffusion treated specimens were pack aluminized to produce a platinum modified aluminide coating. The method used here to aluminize Ni-based superalloy sample is above pack cementation using a single-step high-activity aluminizing technique.

The pack used for aluminizing consisted of 10 wt. % Al powder (50 to $150\ \mu\text{m}$ in particle size) as an aluminum source, 2 wt. % NH_4Cl as the activator, and the balance was 88 wt.% of α -alumina (70 - $210\ \mu\text{m}$) as the inert filler. The mixed pack was then put in a stainless steel cylindrical container with a diameter of 5 cm and a height of 8 cm. The cylinder was filled up to three quarters and the upper quarter of the container was left as the reaction chamber that contained the Inconel sample. The sample was hanged with Pt wire, this wire passed through a hole in the container lid. The container was then filled with Ar and closed with alumina-based cement. This process is known as above pack cementation.

The container was then put in a closed tube furnace with Ar atmosphere. The aluminizing process was carried out at $1034 \pm 5^\circ\text{C}$ for up to 4 hours. After the aluminizing treatment, the specimens were cleaned and weighed to determine the aluminum pickup. No further heat treatment was given to the specimens after aluminizing [14].

Isothermal Oxidation:

Both of the uncoated and coated specimens were isothermally oxidized in dry air at temperature (700 , 800 , 900 , and $1000 \pm 3^\circ\text{C}$) for up to 200 hrs time. The weight changes due to oxidation were monitored continuously using a (Mettler 200) microbalance with a precision of $100\ \mu\text{g}$. The surfaces and cross sections of oxidized samples in air were examined using SEM (FEI/Philips /XL-30 W/TMP). The phases present in the alloys were identified with X-ray with General Electric Diffractometer, operating at scanning speed of $2^\circ (2\theta)$ per minute with Cu k_α ($\lambda = 1.54$).

Results and Discussion

Microstructure of Pt-Modified Aluminide Coating:

The microstructure of platinum aluminide coating on inconel alloy 600 that is termed coated system in the present study is shown in Fig. 1. The platinum aluminide coating reveals a three layer structure in the as aluminized condition: the outer layer has a two phase structure in which the PtAl_2 phase (bright grains) is distributed in a NiAl matrix (dark grains) as shown in Fig.1 (b). This structure of the outer coating layer is expected, based on the extensive interdiffusion between the substrate and the Pt layer that takes place during the prior diffusion treatment. The PtAl_2 phase fully constituted the outer coating when prior diffusion treatment was done at 850°C for 0.5 hr. This inter-metallic phase is known to be extremely brittle, perhaps much more so than the β - NiAl phase [11]. The distribution of the PtAl_2 phase in β - NiAl matrix takes place as the temperature of diffusion treatment is

increased to 1034 °C for up to 2 hrs. The other two underlying layers of this coating are: intermediate β-NiAl layer and the inner interdiffusion layer.

Oxidation of Uncoated Inconel in Air:

The weight gain data during isothermal oxidation in dry air for the uncoated system at a temperature range of 700-1000 °C for up to 200 hrs is plotted in Fig. 2. The oxidation kinetics can be described by examining the growth rate time constant or *n* value, which is found as the exponent in the following rate equation:

$$\left(\frac{\Delta W}{A}\right) = k t^n \quad (1)$$

where Δw is the weight gain, *A* is the sample surface area, *k* is the rate constant, and *t* is time. Values of *n* are shown in table 2. It is found that the relationship is parabolic where *n* = 0.5. Deviation from theoretical value of *n* = 0.5 can be explained by an oxide layer cracking, leading to a sudden increase of the surface area in contact with oxygen and thus to an acceleration of the oxidation kinetics. These results have shown that the parabolic kinetics at this temperature range can be quantified on the modified parabolic rate law with the assumption that oxidation is controlled by diffusion mechanism and the grain boundaries are the only effective short-circuit diffusion paths [15]. The grain boundary diffusion mechanism provides an initially high oxidation rate. As time passes, oxide grain growth occurs, which decreases the number of easy diffusion paths and slows the oxidation rate. Therefore, the easy pathways are cut off, and the oxidation rate is decreased beyond that for parabolic kinetics.

For the parabolic kinetics, the rate equation takes the form:

$$\left(\frac{\Delta W}{A}\right)^2 = k_p t \quad (2)$$

where *k_p* is the parabolic rate constant in units of (mg²/cm⁴.sec). The parabolic oxidation rate constant for four series of experiments are calculated and the linear lines are represented in Fig.3 as the least squares curve fits to the data. The parabolic oxidation rate constants (*k_p*) for the set of experiments are listed in the table 2.

The parabolic oxidation rate constant of inconel alloy 600 in air, vary by one order of magnitude from a low of 1.43 * 10⁻⁷ (mg²/cm⁴.sec) at 700 °C to a high of 2.37 * 10⁻⁶ (mg²/cm⁴.sec) at 1000 °C. The data in table 2 are single-temperature rate constants and, for practical applications, should be generalized over the entire range of temperatures. The following Arrhenius equation relates the oxidation rate to temperature:

$$k_p = A \exp\left[-\frac{B}{RT}\right] \quad (3)$$

where *A* and *B* are constants, *R* is the universal gas constant, and *T* is the temperature in K. In thermodynamic sense, *B* would be the activation energy but, in the present formulation, that will not be the case. In order to evaluate the appropriate ranges of temperatures over which to fit *k_p* as a function of temperature, the values in table 2 were plotted vs. (1/*T*) as shown in Fig. 4. A linear regression analysis of the form of Eq. (3) results in the following relationships for *k_p* as a function of temperature:

$$k_p = 2.6 \times 10^{-1} \exp\left[-14025.8 / T\right] \quad T \in (973 \text{ K}, 1073 \text{ K}) \quad (4a)$$

$$k_p = 3.6 \times 10^{-3} \exp\left[-9438.44 / T\right] \quad T \in (1073 \text{ K}, 1173 \text{ K}) \quad (4b)$$

$$k_p = 1.3 \times 10^{-2} \exp [-10668.7/T] \quad (4c)$$

The values of k_p so calculated are in units of ($\text{mg}^2/\text{cm}^4 \cdot \text{sec}$). When k_p from Eq. (4) is used in Eq. (2), the square of the oxygen weight gain per unit surface area over the time interval of oxidation is computed as (mg^2/cm^4).

At low temperatures, Inconel alloy 600 experiences a period of transient oxidation for approximately 30 hours of oxidation in air followed by parabolic oxidation at a greatly reduced rate. In other words, data reveal a parabolic oxidation rate (k_p) that obeys an Arrhenius-type equation of the form:

$$k_p = k_0 e^{-\frac{Q}{RT}} \quad (5)$$

where k_0 is the pre-exponential factor, Q is the activation energy, T is the temperature, and R is the universal gas constant $8.33 \text{ (J / K) / mol}$. From the experimental data, the activation energy was calculated from a plot of $\log (k_p)$ vs $(1/T)$ in the temperature range from 700°C to 1000°C as shown in Fig. 5. The value obtained for the parabolic growth of Cr_2O_3 was 105 kJ mol^{-1} , which is in good agreement with values in the literature, $100\text{-}170 \text{ kJ mol}^{-1}$, on Ni-20Cr alloys [16].

At low temperature (i.e., 700°C) the oxide scale was too thin to be detectable with X-ray diffraction analysis. The main phases that exist on inconel alloy 600, as long as those are present in sufficient amount are NiO, and spinel phases of Ni (Cr_2O_4 , Fe_2O_4). At 700°C , an external layer of NiO (which is formed by the outward diffusion of Ni toward oxide-gas interface and inward diffusion of O) and a complex spinel Ni (Cr, Fe) $_2$ O $_4$ are formed. A nearly continuous layer of Cr_2O_3 lies below. In the case

of Ni-Cr and Ni-Al oxidation [15], even fast diffusion along grain boundaries is still apparently too slow to account for the measured oxide growth rates. Short circuit diffusion of oxygen appears to occur to a greater or lesser extent in practically all oxide films. Consequently, oxygen is transported as molecules along short circuit pathways. This inward oxygen gas transport is responsible for the growth of new oxide within the films and for the growth of the inner layer of the well-developed duplex films, which grow on the alloy.

The oxide surface was examined using SEM as shown in Figs. 6-9. The scale appears similar to numerous nodules on the surface and no indication of scale spallation or cracking. Nodules of NiO nucleated on the surface and grew with a duplex structure. The nucleation increased with increasing temperatures so that the nodules nucleated at lower temperature are slightly larger and less dense, whereas at higher temperatures, the nodules become smaller and denser. Subsequent mass gain may result from the nucleation and formation of more nodules. One interesting feature of the nodules is that the gas/surface appears to have porosity (backscatter image Fig. 6c). Cross section micrograph is presented in Fig. 8, which reveals the presence of many cavities under the oxide layer. This corresponds to Cr depletion of inconel alloy 600 by the outward diffusion of Cr toward the oxide layer.

Generally, the oxidation mechanism of a commercial Inconel alloy 600 is similar to that of Ni-Cr alloys [17, 18, 19, and 20] and subsequent steps show an interesting difference between the two alloys due to the effect of the minor alloying

component iron in inconel alloy 600. It is the available iron, which combines preferentially with the nickel oxide to form a NiFe_2O_4 spinel phase possibly because of the higher diffusion rate of iron and the higher formation rate of NiFe_2O_3 . As the oxide layer grows thicker, the solid-state reaction between NiO and $\alpha\text{-Fe}_2\text{O}_3$ induces the formation of a mixture of NiFe_2O_3 and NiO (the outermost layer is enriched in nickel ferrite). Cr_2O_3 appears at the interface between the alloy matrix and the outer layer rich in nickel oxides. So, the scale corresponds to the duplex system $\text{NiO} + \text{NiFe}_2\text{O}_3 / \text{Cr}_2\text{O}_3 / \text{alloy}$. When the Cr_2O_3 sub-layer is continuous, the NiO layer stop growing and the oxidation kinetics hardly reflect the growth of the Cr_2O_3 layer.

At 900 °C, the continuous Cr_2O_3 sub-layer has grown and the reaction has progressed and NiO has not been observed at this condition. Either the whole NiO layer has reacted with Cr_2O_3 to form NiCr_2O_4 , or it has peeled off during oxidation.

Oxidation of Coated System:

The kinetic behavior of Inconel alloy 600 with Pt -modified aluminide coating in air during isothermal oxidation at 800 and 900 °C for 200 hours follows the parabolic rate. The values of the parabolic rate constant k_p and n , in the coated system are determined in the same procedure followed in the previous work and listed in the Table 3 .The value of k_p obtained at 900 °C is $k_p = 6.63 \times 10^{-7}$ and about half that for the uncoated Inconel alloy 600 ($k_p = 1.16 \times 10^{-6}$) ($\text{mg}^2/\text{cm}^4 \cdot \text{sec}$).

The data for the Inconel alloy 600 obtained in the case of oxidation in air suggest that this undergoes oxidation according to the parabolic law only

after an initial transition period of ~ 30 hours. Krishna et.al [21] studied the isothermal oxidation characteristics of Ni-Cr-Al alloys between 1000 and 1200 °C at 0.1 atm of oxygen. They observed that all the Ni-Cr-Al alloys go through an initial transient period, lasting up to 20 hours for certain composition.

The first stage of the coating degradation in the coated system is the transformation of the top phase structure ($\text{PtAl}_2 + \beta\text{-NiAl}$) to the single phase $\beta\text{-NiAl}$. The second stage is the transformation of $\beta\text{-NiAl}$ to $\beta\text{-NiAl} + \gamma'$. The major oxide phases present here are the more stable alumina ($\alpha\text{-Al}_2\text{O}_3$), NiAl_2O_4 , Cr_2O_3 , and Fe_2O_3 emerging after 200 hrs oxidation period at 900 °C in air. Moreover, the mechanism of void formation can be explained as follows: when the transformation from $\beta\text{-NiAl}$ to γ' occurs by front growing into the middle of the outer zone (inward β to γ' transformation due to Al consumption at the surface and outward transformation due to the outward Ni diffusion from the substrate), voids may be formed due to vacancy coalescence mechanism .

In general, the values of k_p indicate that the modification of aluminide coating with platinum on Inconel alloy 600 results in a significant improvement in the oxidation resistance. The changes that take place in phase constitution of coated system during the isothermal oxidation in air have been less lightening because of the complexity of such systems and need high accurate facilities.

Conclusions

From the Isothermal oxidation tests in air at temperatures 700 to 1000 °C; the following results can be concluded:

1- Inconel alloy 600 exhibits steady parabolic diffusion controlled oxidation rate dependence in air over the temperatures 900 and 1000 °C for long time intervals up to 200 hours.

2- At 700 and 800 °C, Inconel alloy 600 experiences a period of transient oxidation for approximately 30 hours.

3- At 700 and 800 °C, no oxide spalling was found.

4- The parabolic rate constant (k_p) varies by one order of magnitude from a low value of $k_p = 1.43 \times 10^{-7}$ at 700 °C to a high value of $k_p = 1.43 \times 10^{-6}$ ($\text{mg}^2/\text{cm}^4 \cdot \text{sec}$) at 1000 °C.

5- The activation energy for Inconel alloy 600 is estimated to be 105 kJ/mole.

6- The major oxide layers formed on Inconel alloy 600 are: Cr_2O_3 , NiCr_2O_4 , and NiFe_2O_4 as identified by X-ray diffraction analysis.

7- The coated system exhibits good oxidation resistance in air compared with Inconel alloy 600 at the same identified conditions and oxidation kinetics follow the parabolic oxidation rates.

References

1. Chan W.Y, Evans H.E, et.al., "The Influence of NiAl_3 on the High Temperature Oxidation of a Plasma-Sprayed Overlay Coating", *Mat. at High Temp.*, Vol.17, No.2, PP.173-178, 2000
2. Bianco R., Rapp R. A., "Pack Cementation Aluminide Coatings on Superalloys: Co-deposition of Cr and Reactive Elements", *J. Electrochem. Soc.*, Vol. 140, No. 4, pp.1181- 1190, April 1993 .
3. Das D. K., Singh V., Joshi S. V., "Evolution of Aluminide Coating Microstructure on Nickel-Base Cast Superalloy CM-247 in a Single Step High-Activity Aluminizing Process", *Meta. And Mater. Trans. A*, Vol. 29A, pp. 2173-2188, August 1998.
4. Moon D.P, "Role of Reactive Elements In Alloy Protection", *Mater. Sci. and Tech.*, Vol.5, PP.754-764 August 1989.
5. Angenete J., "Microstructure of Pt Modified Aluminide Diffusion Coatings Ni Based Single Crystal Superalloys", Ph.D. Thesis, Chalmers- Goterborg University, Sweden, 1999.
6. Diego S., Highway K., "The Effect of Rh % on the Oxidation Resistance of Platinum Rhodium Modified Aluminide Coatings on Mar M-509 and FSX-414 cobalt base alloys", TMS Annual Meeting, 1997 .
7. Zhang Y., Haynes J. A., Lee W. Y., Wright et.al., "Effect of Pt Incorporation on the Isothermal Oxidation Behavior of Chemical Vapor Deposition Aluminide Coatings", *Metall. & Mat. Trans. A*, Vol. 32A, pp. 1727-1741, July 2001.
8. Moosa A. A., "Mechanism of Oxide Adherence on Ni-0.1 wt % Ce", *Eng. Tech. Suppl. of No. 4*, Vol. 20, pp. 19- 29, 2001.
9. Moon D. P., "Role of Reactive Elements in Alloy Protection", *Mat. Sci. and Tech.*, Vol. 5, pp. 754-764, August 1989.
10. Stringer J., "The Reactive Element Effect in High Temperature Corrosion", *Mat. Sci. and Eng.*, 120A, 129-137, 1989.
11. Das D. K., Singh V., Joshi S. V., "Effect of Al Content on

- Microstructure and Cyclic Oxidation Performance of Pt-Aluminide Coatings", *Oxid. of Met.*, Vol. 57, Nos. 3/4, pp. 245-266, 2002.
12. An T. F., Guan H. R., et al., "Effect of θ - α - Al_2O_3 Transformation in Scales on the Oxidation Behavior of a Nickel-Base Superalloy with an Aluminide Diffusion Coating", *Oxid. of Met.*, Vol. 54, Nos. 3/4, pp. 301-316, 2000.
 13. Stott F. H., Gleeson B., Castello P., "The Effect of Pt Additions on the Oxidation of Directionally-Solidified Ni-Cr-Al-Y- Cr_3C_2 Alloys at 1100 and 1200 °C", *Mat. at High Temp.*, 16 (1) 15-26, 1999.
 14. Al-Hatab, Khalil, "Effect of Environments on Oxidation Behavior of Inconel Alloy 600", Ph.D. Thesis, University of Technology, Iraq 2004.
 15. Kyung H., Kim C. K., "Microstructure Evolution of Duplex Grain Structure and Interpretation of the Mechanism for NiO Scales Grown on Pure Ni-and Cr-Doped Substrate During High Temperature Oxidation", *Mat. Sci. and Eng.*, B76, pp. 173-183, 2000.
 16. Salmon C., Tiberghien D., et al., "Oxidation Behavior in Air of Thin Alloy 601 Fibers", *MATH*, Vol. 17, No. 2, pp. 271-278, 2000.
 17. Strehl G., Borchardt G., "On Deviations from Parabolic Growth Kinetics in High Temperature Oxidation, "www.imet.tu-clausthal.de/agbor/users/gstrehl/publications/macc2001.pdf.
 18. McIntyre N. S., Zetaruk D., Owen G., D., "XPS Study of the Initial Growth of Oxide Films on inconel 600 Alloy", *Application of Surf. Sci.*, Vol. 2, pp. 55-73, 1978.
 19. Panter J., Viguier B., Andrieu E., "Microstructural Evolution of Alloy 600 During Dry Oxidation", *Mat. Sci. Forum*, Vols. 369-372, pp. 141-148, 2001.
 20. Gourgues A. F., Andrieu E., "Oxidation Assisted Creep of Alloy 600", *J. Phys. IV France* 9, pp. Pr9-297-Pr9-303, 1999.
 21. Krishna G. R., Das D. K., et al., "Role of Pt Content in the Microstructural Development and Oxidation Performance of Pt-Aluminide Coatings Produced using High-Activity Aluminizing Process", *Mat. Sci. and Eng.* A251, 40-47, 1998.

Table 1. : Nominal composition of Inconel alloy 600.

Chemical Limits								
Ni	Cr	Cu	Fe	Mn	Si	S	P	C
72.0	15.5	0.5	8.0	1.0	0.5	0.015	0.015	0.065
Min.		Max.		Max.	Max.	Max.	Max.	

Table 2: *n* values & parabolic oxidation rate coefficients k_p for oxidation of inconel alloy 600 in air for up to 200 hours.

Temperatures (°C)	<i>n</i> values	k_p (mg ² /cm ⁴ .sec)
700	0.5	$1.43 * 10^{-7}$
800	0.56	$5.48 * 10^{-7}$
900	0.49	$1.16 * 10^{-6}$
1000	0.49	$2.37 * 10^{-6}$

Table 3: *n* values & parabolic oxidation rate coefficients k_p for oxidation of coated system.

Environment	800°C k_p (mg ² /cm ⁴ .sec) <i>n</i>	900°C k_p (mg ² /cm ⁴ .sec) <i>n</i>
Air	$3.08 * 10^{-7}$ 0.56	$6.63 * 10^{-7}$ 0.44

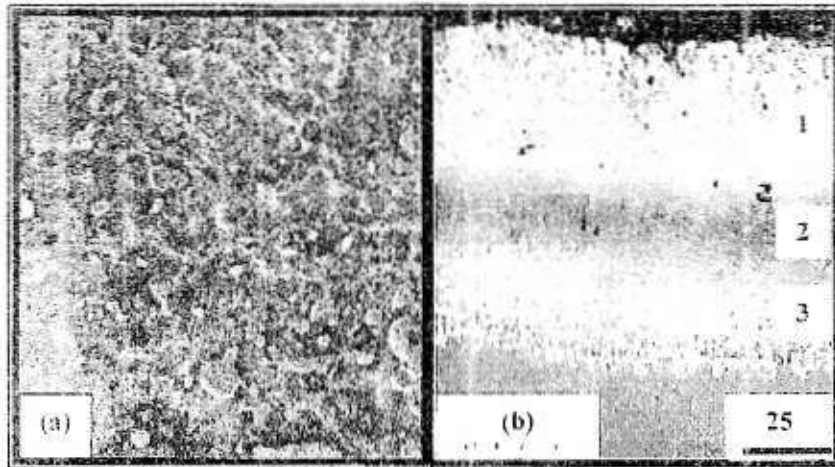


Fig.1 SEM images of Pt -Modified Aluminide Coating in the as coated. (a) Top view (X500), and (b) Cross section view, 1: $PtAl_2 + \beta-NiAl$, 2: $\beta-NiAl$, and 3: inter-diffusion zone.

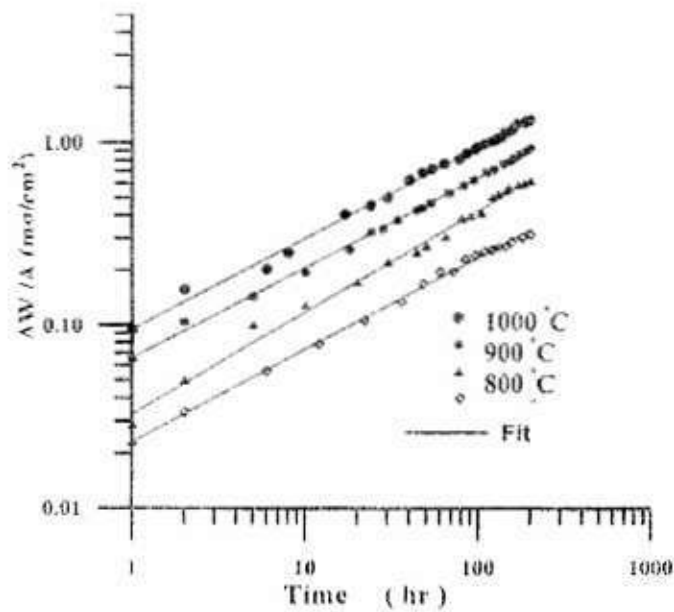


Fig.2 Typical log-log plots of oxidation weight-gain data for inconel alloy 600 oxidized in air at temperatures range 700-1000 °C for up to 200 hour.

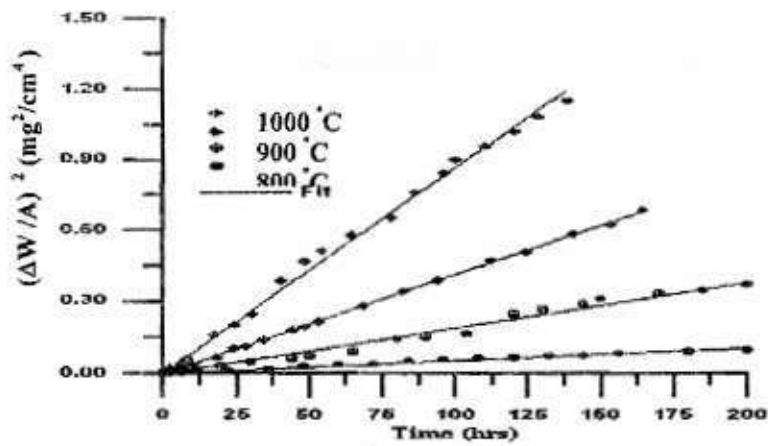


Fig. 3 Square of the weight gain/unit area vs. time for inconel alloy 600 oxidized in air at temperatures range 700-1000 °C for up to 200 hour.

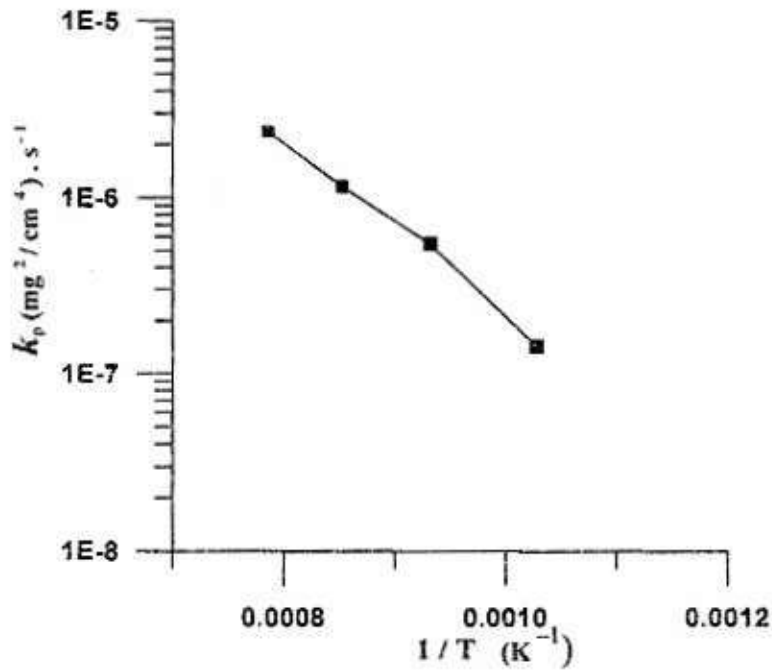


Fig.4 Correlations of the parabolic rate coefficients k_p vs. $1/T$ for inconel alloy 600 oxidized in air.

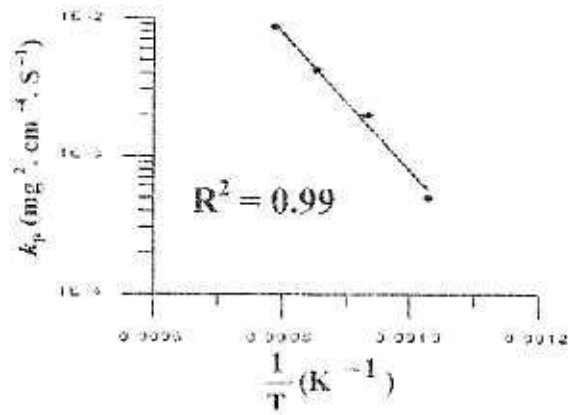


Fig. 5 Plot of K_p vs $1/T$ for isothermal oxidation of inconel alloy 600 in air.

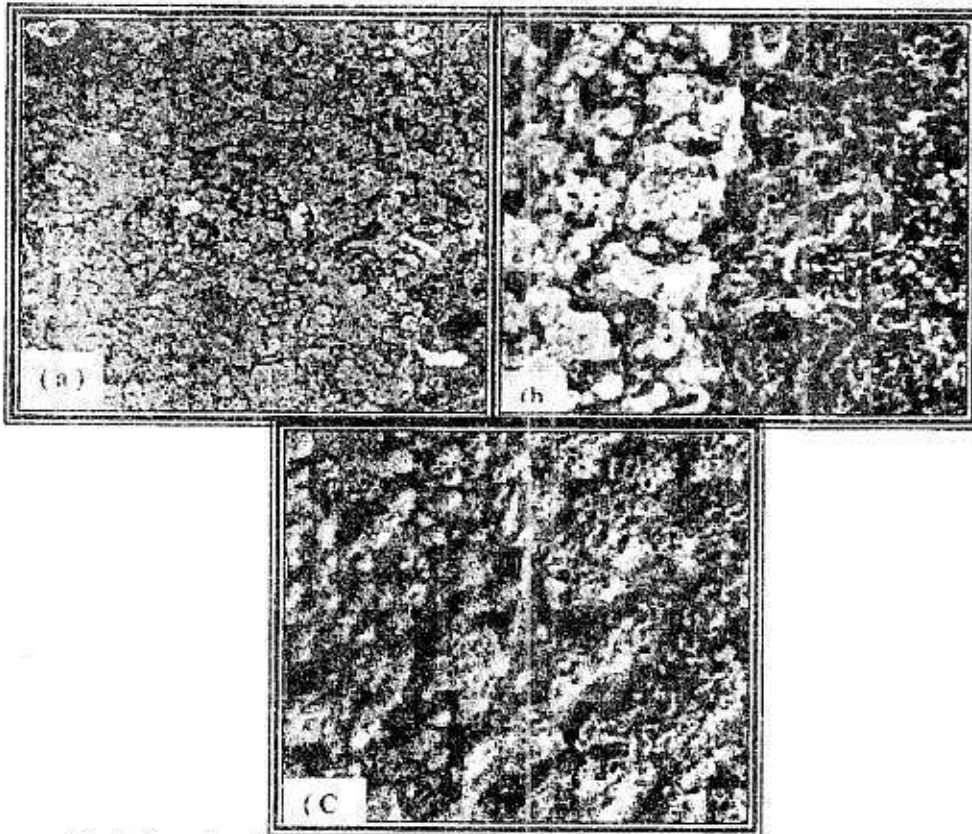


Fig.6 Scanning electron micrograph of surface oxide growth on inconel alloy 600 oxidized in air at 700 °C for up to 200 hr. (a) Top view (X200), (b) top view (X500), and (c) backscatter image (X500).

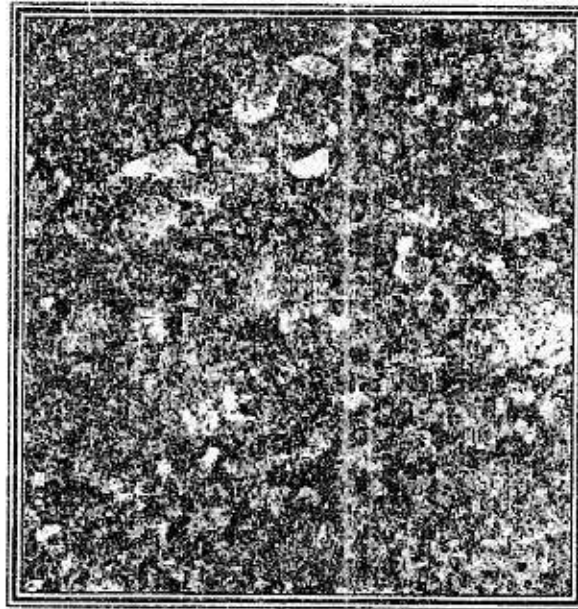


Fig.7 Scanning electron micrograph of surface oxide of inconel alloy 600 oxidized in air at 1000 °C for up to 200 hr (X500).

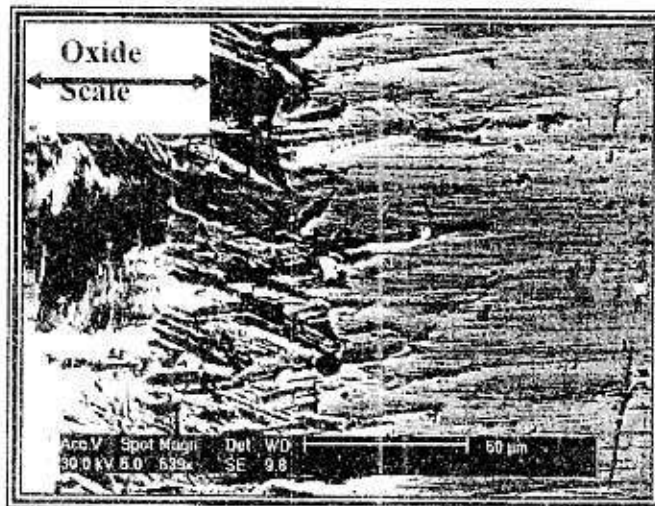


Fig.8. Tansverse section image of SEM of inconel alloy 600 oxidized in air at 1000 °C for up to 200 hours.

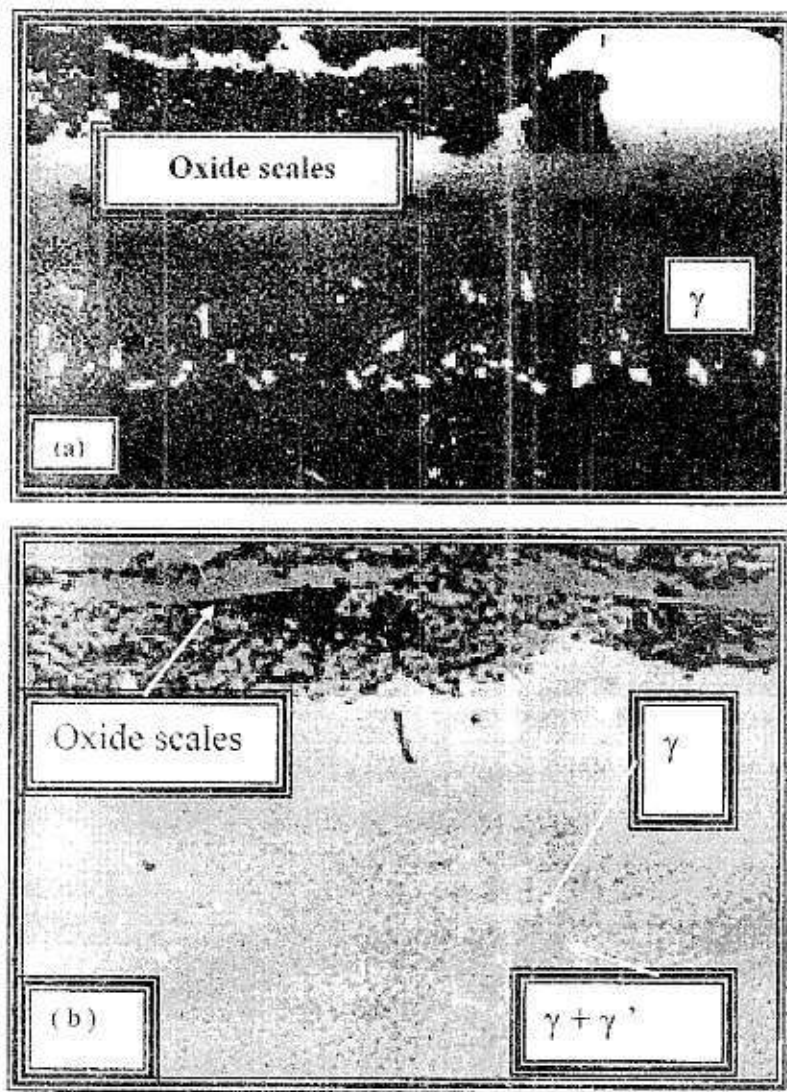


Fig. 9 Transverse cross image of SEM of coated system oxidation in air for up to 200 hour at: (a) 800 °C, and (b) 900 °C.